ADVANCED MATERIALS INTERFACES
www.advmatinterfaces.de

Designing "Supermetalphobic" Surfaces that Greatly Repel Liquid Metal by Femtosecond Laser Processing: Does the Surface Chemistry or Microstructure Play a Crucial Role?

Jiale Yong, Chengjun Zhang, Xue Bai, Jingzhou Zhang, Qing Yang, Xun Hou, and Feng Chen**

It is demonstrated that the wettability of liquid metal (LM) on a substrate is very different from the water wettability. Superhydrophobic and superhydrophilic silicon and polydimethylsiloxane surfaces, respectively, are obtained by femtosecond laser processing and proper chemical modification. All of the structured surfaces have excellent LM repellence, that is, supermetalphobicity, in spite of superhydrophobicity or superhydrophilicity. The experimental comparison and contact model analysis reveal that surface microstructure actually plays a crucial role in endowing a surface with supermetalphobicity while surface chemistry has a little influence on the formation of supermetalphobicity, because the liquid/solid contact is replaced by a solid/solid contact mode for a LM droplet on a textured substrate. It is believed that the established principle for creating supermetalphobic surfaces will enable to accelerate the application progress of LM materials in flexible circuits and liquid robots.

Liquid metals (LMs), for example, eutectic gallium–indium (EGaIn), have attracted increasing attention because of their important potential applications in liquid robots and flexible circuits.[1–6] The core technology for achieving these applications is to control the shape and adhesion of LM and even obtain complex LM patterns.[7–11] However, LM has the fundamental property of liquid, such as fluidity, and it is easy to adhere to a solid substrate due to the high adhesion between solid surface and LM.[12–15] The high adhesion makes it more difficult to control the LM shape and prepare fine LM patterns. An effective method that can endow a surface with excellent LM repellence is highly desired to apply the LM in liquid robots and flexible circuits. Superhydrophobic surfaces are recently prepared to repel LM in the application of the LM-based circuits.[16–19] The superhydrophobic surfaces with strong water repellence are generally fabricated by the combination of hierarchical surface microstructure and the chemistry with extremely low surface free energy (SFE).[20–23] In fact, LM is very different from water in the aspect of no matter the chemical composition or the physical/mechanical property. Whether there is an equivalence between superhydrophobicity and LM repellence has not been demonstrated or been well revealed until now. The relationship between LM repellence and superhydrophobicity should be clearly clarified for guiding researchers to design LM-repellent structure in a right way. On the other hand, most traditional methods are just able to form LM-repellent microstructures on a special material substrate.[16–19] Those methods are not flexible and universal. Therefore, establishing the principle for endowing any materials with remarkable repellence to LMs has the extremely vital significance, and to date, the preparation of LM-repellent surface by a simple and widely applicable way is really a great challenge in the field of LM applications.

Here, the influence of the surface chemistry and microstructure on the wettability of a solid surface to LM was investigated. Micro/nanoscale structures were prepared on the silicon (Si) and polydimethylsiloxane (PDMS) surfaces by simple femtosecond laser (fsL) processing. After additional chemical modification/treatment, both superhydrophobic and superhydrophilic Si/PDMS surfaces were obtained. We find that all of these structured surfaces have excellent LM repellence in spite of superhydrophobicity or superhydrophilicity. The difference between LM wettability and water wettability of a solid surface was revealed from the aspects of experimental comparison and contact model analysis, with water/LM droplets on different substrates.

Prof. J. Yong, Dr. X. Bai, Dr. J. Zhang, Prof. X. Hou, Prof. F. Chen
State Key Laboratory for Manufacturing System Engineering and Shaanxi Key Laboratory of Photonics Technology for Information
School of Electronics & Information Engineering
Xi'an Jiaotong University
Xi'an 710049, P. R. China
E-mail: chenfeng@mail.xjtu.edu.cn

Prof. J. Yong, Dr. C. Zhang, Dr. X. Bai, Dr. J. Zhang, Prof. Q. Yang, Prof. X. Hou, Prof. F. Chen
The International Joint Research Laboratory for Micro/Nano Manufacturing and Measurement Technologies
Xi'an Jiaotong University
Xi'an 710049, P. R. China
E-mail: yangqing@xjtu.edu.cn

Dr. C. Zhang, Prof. Q. Yang
School of Mechanical Engineering
Xi'an Jiaotong University
Xi'an 710049, P. R. China

The ORCID identification number(s) for the author(s) of this article can be found under https://doi.org/10.1002/admi.201901931.

DOI: 10.1002/admi.201901931

ADVANCED MATERIALS INTERFACES
www.advmatinterfaces.de

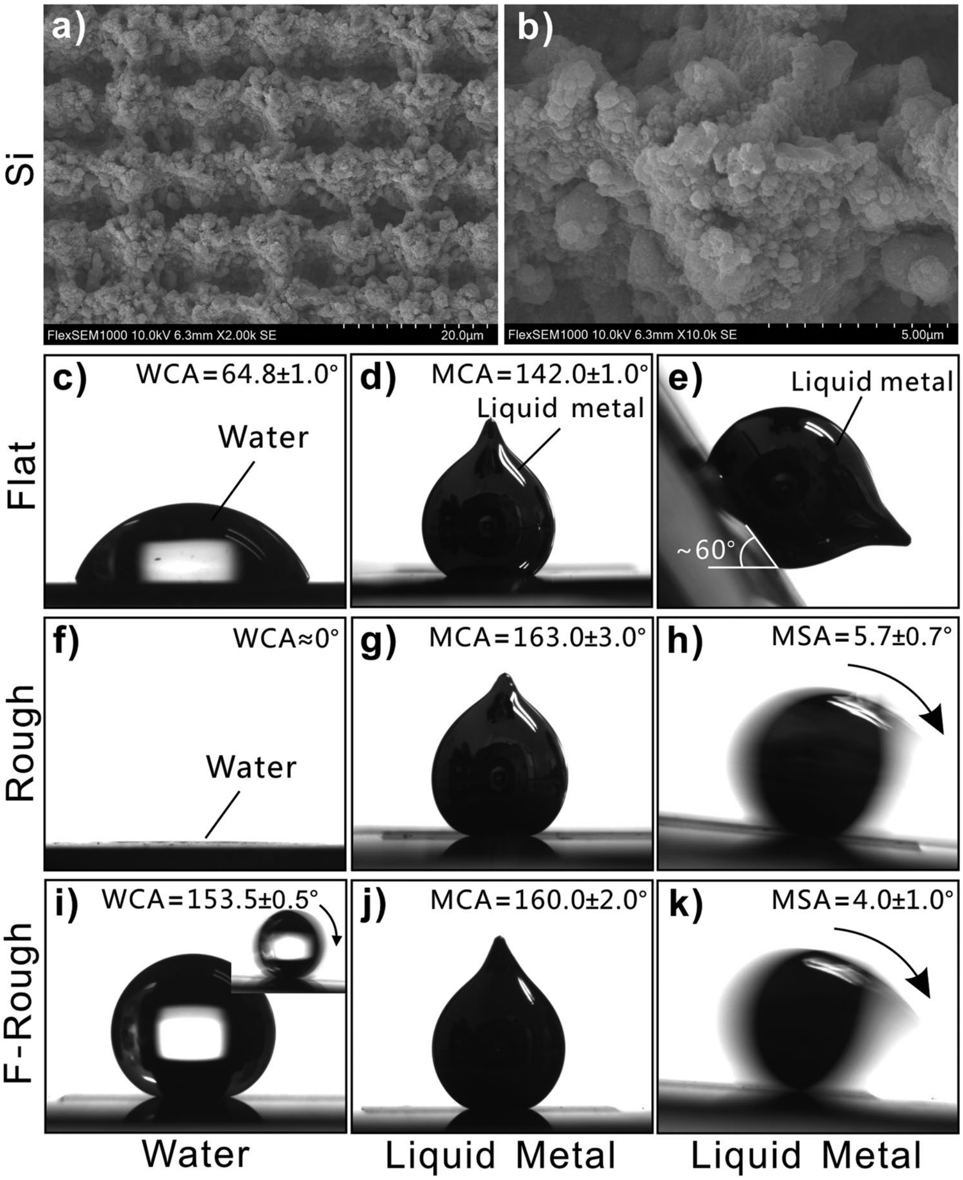

Figure 1. Microstructure and water/LM wettabilities of Si surface. a,b) SEM images of the Si surface ablated by fsL. c–e) Water or LM droplet on the untreated flat Si surface. f–h) Water or LM droplet on the fsL-induced rough Si surface. i–k) Water or LM droplet on the fluorinated rough (F-rough) Si surface. c,f,i) Water droplet on the Si surfaces. d,g,j) LM droplet on the Si surfaces. e,h,k) LM droplet sticking on or rolling off the sample surface. The inset in i) shows the process of a water droplet rolling away.

Si with high SFE and PDMS with low SFE are selected as the substrates in this experiment as they are two typically different materials with opposite wettability. Si is an intrinsically hydrophilic material and its wettability can be transferred to hydrophobic by fluoroalkylsilane modification, while PDMS is an intrinsically hydrophobic material and its wettability can be transferred to hydrophilic via oxygen plasma irradiation. The natural water wettability can be amplified by surface microstructure for a solid material.[24–29] FsL processing was utilized to create microstructure on the Si and PDMS surfaces because it has the capacity of ablating various materials and generating micro/nanoscale structures on those materials.[30–36]

Figure 1a,b is the scanning electron microscope (SEM) images of the Si surface which was ablated by fsL.[37–41] Periodic mountain-like structures was induced on the Si substrate. The mountains are about 6 μm in diameter and 2.9 μm in height. They arrange as an array with the period of 10 μm. Every micromountain is surrounded by four deep microholes with the depth of ≈4.6 μm and there are abundant nanoscale particles coating the surface of the micromountains. The roughness of the laser-ablated surface is 2.46 μm. With regard to the untreated flat Si surface, it shows hydrophilicity to a water droplet with a water contact angle (WCA) of 64.8 ± 1.0° (Figure 1c). When an EGaIn LM droplet was placed on the flat Si surface, the droplet would adhere to the sample and form a round tower-like shape.

The measured metal contact angle (MCA) of this LM droplet is 142.0 ± 1.0° (Figure 1d). A large contact area between the LM droplet and Si substrate can be clearly observed. Until the sample was tilted to ≈60°, the LM could detach from the surface and roll away (Figure 1e), revealing that the flat Si surface exhibits a relatively high adhesion to LM droplet.

When hierarchical microstructure was prepared on the Si surface by fsL treatment, the rough Si surface was enhanced to superhydrophilic. Water droplet on the rough Si surface could spread out and fully wet the structured area (Figure 1f). The final WCA was near to 0°. In comparison to the untreated flat substrate, the MCA of a LM droplet on the rough Si surface is distinctly increased to 163.0 ± 3.0° (Figure 1g). Meanwhile, the touch area between the LM and the Si substrate has an obvious decrease. The LM droplet would roll away once the surface was tilted to 5.7 ± 0.7°. That is, the metal sliding angle (MSA) was only 5.7 ± 0.7° (Figure 1h), which is different from the water droplet on such surface. Such high MCA value and low MSA value indicate that the fsL-structured rough Si surface shows excellent LM repellence.

Following the definition of the term “super-hydro-phobicity,” we can use the newly coined word “super-metal-phobicity” to define the property that a LM droplet has the MCA higher than 150° and the MSA smaller than 10° on a solid surface. Therefore, the Si surface has supermetalphobicity after fsL processing.

The SFE of the fsL-induced rough Si sample was lowered by fluoroalkylsilane modification. After that, the fluorinated rough (F-rough) surface became superhydrophobic. Water droplet could maintain a spherical shape with a WCA of 153.5 ± 0.5° on the F-rough surface (Figure 1i). Ultralow water adhesion was also exhibited and the water droplet would easily roll-off on the F-rough Si surface when the sample was slightly shocked (Inset of Figure 1i). Interestingly, LM droplet has a MCA of 160.0 ± 2.0° on the F-rough Si surface, demonstrating excellent supermetalphobicity of the sample surface. (Figure 1j). As the F-rough surface was tilted to 4.0 ± 1.0°, the LM droplet could quickly roll-off (Figure 1k).

It is found that both the superhydrophilic (rough) and the superhydrophobic (F-rough) Si surfaces have similar supermetalphobicity. That is, the supermetalphobicity does not depend on the superhydrophobicity or superhydrophilicity for a solid substrate. Such conclusion was also verified on a PDMS substrate whose intrinsic SFE is very low in comparison to the high-SFE Si surface. By using the same process of ablating Si surface to process a PDMS surface, hierarchical microstructure was also induced on the PDMS surface after fsL processing (**Figure 2**a,b).[42–46] Original PDMS is hydrophobic with the WCA of 104.5 ± 3.5° (Figure 2c). The MCA of a LM droplet on the flat PDMS was just 142.5 ± 0.5° (Figure 2d), revealing common metalphobicity of the PDMS substrate. The untreated PDMS surface shows extremely high adhesion to LM, as a LM droplet was able to firmly stick on the untreated PDMS sample that was placed vertically (Figure 2e). For the fsL-induced rough PDMS, it exhibits superhydrophobicity and extremely low water adhesion with the WCA of 155.7 ± 1.7° for a water droplet on such surface (Figure 2f). LM droplet on the surface has a MCA of 158.3 ± 4.3° (Figure 2g) and could roll-off as the sample was slightly tilted (MSA = 4.0 ± 1.0°) (Figure 2h). Therefore, the fsL-structured PDMS surface has remarkable repellence to LM. The PDMS surface was endowed with supermetalphobicity besides superhydrophobicity by the fsL-induced microstructures.

Generally, the PDMS surface can be turned from hydrophobicity to hydrophilicity by short time oxygen plasma irradiation, without changing its morphology. Oxygen plasma is able to activate PDMS and induce radical −SiOH groups on its surface; that is, the hydrophilic $-CH_3$ group of PDMS is transformed to hydrophilic −OH group.[47–50] As the rough PDMS surface was treated by oxygen plasma, the resultant oxygen plasma treated rough surface (O-rough surface) became superhydrophilic. The WCA of a water droplet on the resultant surface finally closed to 0° (Figure 2i). Different from the dramatic conversion of water wettability, the oxygen plasma irradiation has no effect on the wetting behavior of LM on the fsL-textured PDMS surfaces. The same as the rough surface, the O-rough PDMS surface also shows great supermetalphobicity with the MCA of 161.7 ± 1.7° (Figure 2j) and the MSA of 3.3 ± 0.7° (Figure 2k). The results reveal that the fsL-produced rough PDMS surface exhibits superhydrophobicity and the O-rough PDMS surface exhibits superhydrophilicity, whereas both these two kinds of surfaces have excellent repellence or supermetalphobicity to LM.

The adhesion between LM droplet and different sample surfaces was also accurately investigated by the adhesive force measurement. As shown in **Figure 3**, the adhesive force between a LM droplet and the untreated flat Si surface was measured to be 247.70 μN, revealing the Si substrate has a high adhesion to LM. The adhesive force is reduced by more than 100 times after the formation of hierarchical microstructure on the Si surface. No matter the rough superhydrophilic Si surface or the F-rough superhydrophobic Si surface shows very low adhesion to a LM droplet with the measured adhesive forces of only 1.78 and 1.28 μN, respectively. Similarly, the untreated flat PDMS surface exhibits high adhesion to a LM droplet with the adhesive force of 365.32 μN, while the adhesive force between a LM droplet and PDMS substrate was decreased to 1.08 μN for the rough superhydrophobic PDMS surface and 1.26 μN for the O-rough superhydrophilic PDMS surface.

The experimental results indicate that not only the superhydrophobic Si/PDMS surfaces but also the superhydrophilic Si/PDMS surface may show LM repellence. There is no an equivalence between supermetalphobicity and superhydrophobicity. Usually, the cooperation of surface chemistry and morphology determines what water wettability a solid surface has.[20–29,51,52] For example, the fsL-structured Si surface is superhydrophilic while the fsL-structured PDMS surface is superhydrophobic. By contrast, the supermetalphobicity can be achieved on both hydrophilic Si substrate (with high SFE) and hydrophobic PDMS substrate (with low SFE). Even though the fsL-structured Si and PDMS surfaces were further treated by fluoroalkylsilane modification and oxygen plasma irradiation, respectively, the surfaces still maintained their strong repellence to LM, which is independent of the dramatic superhydrophilicity–superhydrophobicity conversion. Therefore, the chemistry of a solid substrate does not seem to have great influence on the formation of supermetalphobicity. Both the untreated Si surface and PDMS surface shows high adhesion to LM, while these surfaces greatly repels LM after fsL processing, demonstrating that

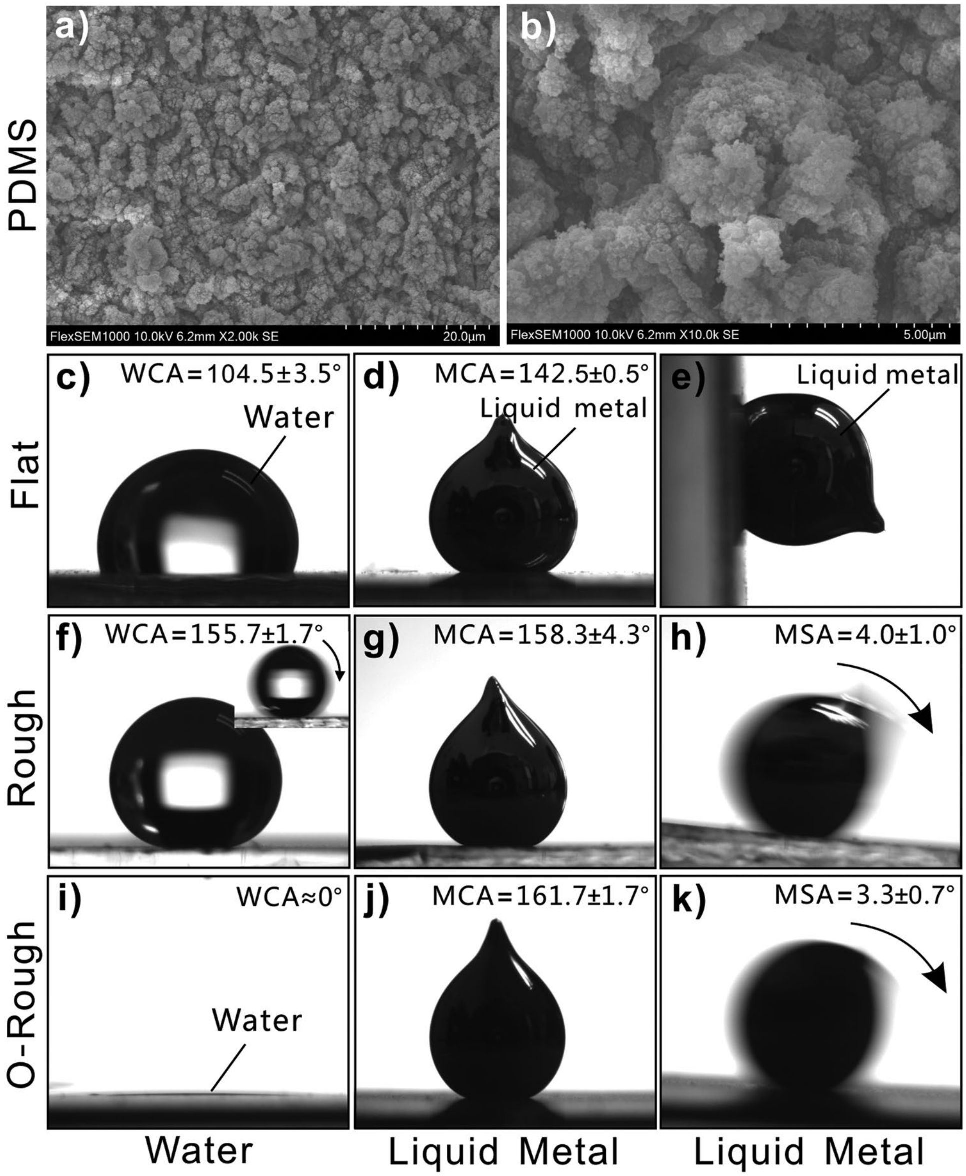

Figure 2. Microstructure and water/LM wettabilities of PDMS substrate. a,b) SEM images of the fsL-ablated PDMS surface. c–e) Water or LM droplet on the untreated flat PDMS substrate. f–h) Water or LM droplet on the fsL-structured rough PDMS surface. i–k) Water or LM droplet on the oxygen plasma treated rough (O-rough) PDMS surface. c,f,i) Water on the sample surface. d,g,j) LM droplet on the sample surface. e,h,k) LM droplet sticking on or rolling off the sample surface. The inset in f) shows the process of a water droplet rolling away.

the surface microstructure plays a crucial role in endowing the surfaces with supermetalphobicity.

Figure 4 depicts the wetting model of a water droplet or a LM droplet on different substrates with high SFE (hydrophilic) or low SFE (hydrophobic), respectively. Water droplet is at the Young wetting state on the hydrophilic flat Si surface,[24,53] with WCA smaller than 90° (Figure 4a). Rough microstructure usually makes inherently hydrophilic surface become more hydrophilic. As the Si surface is ablated by fsL to form hierarchical microstructure, hydrophilicity is enhanced because the surface area of the Si substrate is greatly increased. Water can fully wet the resultant microstructure and is in agreement with the Wenzel wetting state,[24,54] so the rough Si surface presents superhydrophilicity (Figure 4b). In general, there is a passivating oxide layer with thickness of a few nanometers coating the LMs in the presence of oxygen.[12–15] The fluidity and wettability of the LM is significantly affected by this elastic oxide layer. The surface yield stress of the thin oxide layer reaches up to ≈0.4–0.6 N m^{-1}.[16] Only when the applied stress is higher than this critical value, the outside oxide layer ruptures and allows the inside LM to flow out; thereby the LM can penetrate into the void space of rough structure. If a LM droplet is dripped onto the rough Si surface, the outside oxide layer will be first in contact with the tips of the surface microstructure. Because of the very large surface yield stress of the oxide layer, the microstructure peaks are difficult to pierce through the elastic oxide shell. In fact, the contact between LM and rough Si surface occurs at the interface of solid oxide shell and solid Si microstructure; that

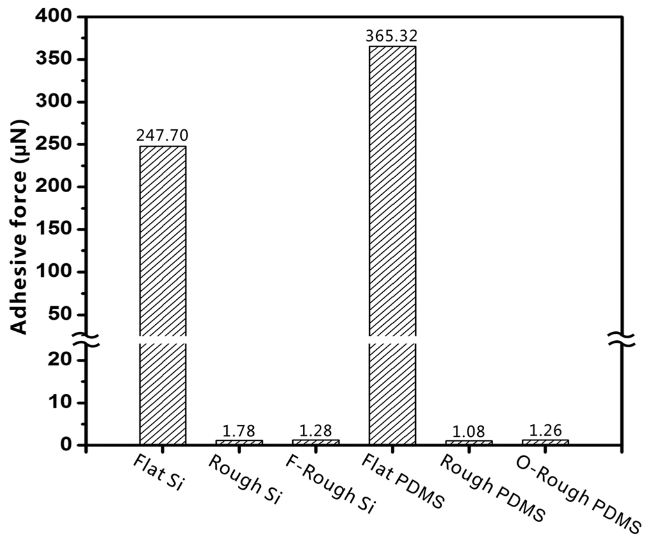

Figure 3. Adhesive force between a LM droplet and different kinds of sample surfaces.

is, the liquid/solid contact is replaced by a solid/solid contact (Figure 4c). As a result, LM is unable to penetrate into and further wet the rough microstructure of Si surface, so the LM is repelled by the rough surface. The contact between LM and the fsL-induced Si microstructure can be considered as the Cassie wetting state,[24,55] although the elastic oxide shell rather than the inside LM directly touches the substrate (Figure 4c).

With regard to a PDMS substrate, it inherently shows hydrophobicity (Figure 4d). The hydrophobicity is amplified to superhydrophobicity by fsL-induced surface microstructure. The rough PDMS surface has excellent superhydrophobicity. In agreement with the Cassie wetting state, water droplet only contacts the peaks of the rough PDMS microstructure (Figure 4e). An air cushion is trapped between PDMS substrate and water. The same as the case of rough Si surface, the PDMS microstructure is also unable pierce through the elastic oxide shell. The existence of the oxide layer prevents the LM from directly touching the PDMS surface. Therefore, the LM is also at the Cassie state on the rough PDMS surface (Figure 4f). The solid/solid contact resulting in a very low adhesion between LM and PDMS surface, so the rough PDMS surface exhibits great LM repellence.

The solid/solid contact manner between LM and solid substrate makes the LM wettability different from water wettability. No matter the low-SFE surface or the high-SFE surface can actually touch the outside oxide layer rather than the inside LM. LM cannot directly touch the solid substrate, therefore, the surface chemistry of substrate has a little effect on the wetting behavior of LM. On the contrary, surface microstructure can significantly reduce the LM/substrate contact area, leading to a very low LM adhesion. Both the experimental result and the wetting model analysis reveal that surface microstructure plays a crucial role in achieving supermetalphobicity.

Weather a LM film can penetrate into the surface microstructure or not is greatly determined by the scale of the microstructure, the thickness of the LM layer, the LM wettability, and the surface tension of oxide metal layer. To simplify the model, we consider the simplest case that LM on the substrate with uniform circular deep holes, as shown in Figure 4g. An intrusion pressure (ΔP) must be exceeded before LM will penetrate into the pores, which can be expressed as:[56–58]

$$\Delta P = \frac{2\gamma}{R} = -\frac{l\gamma\cos\theta_{\text{adv}}}{S} \approx -\frac{4\gamma\cos\theta_{\text{adv}}}{D} \quad (1)$$

where γ is the surface tension of the outside oxide LM layer, R is the radius of the LM meniscus, l is the perimeter of the pores, θ_{adv} is the advancing MCA of LM on the substrate, S is the area of the pores, and D is the pore diameter. ΔP has positive correlation with γ. Since the surface tension of oxide LM is far higher than that of water, so the LM is very difficult to penetrate into the space between surface microstructure compared to water. On the other hand, this equation reveals that a smaller diameter of the micropores will give rise to a higher intrusion pressure. That is, the smaller the scale of the surface microstructure, the more difficult the LM is able to wet the structured surface. According to some estimates, the scale of surface microstructure needs less than a few hundred micrometers to achieve supermetalphobicity for a solid substrate.

The supermetalphobic microstructure has many potential applications, such as reducing the adhesion at the interface of

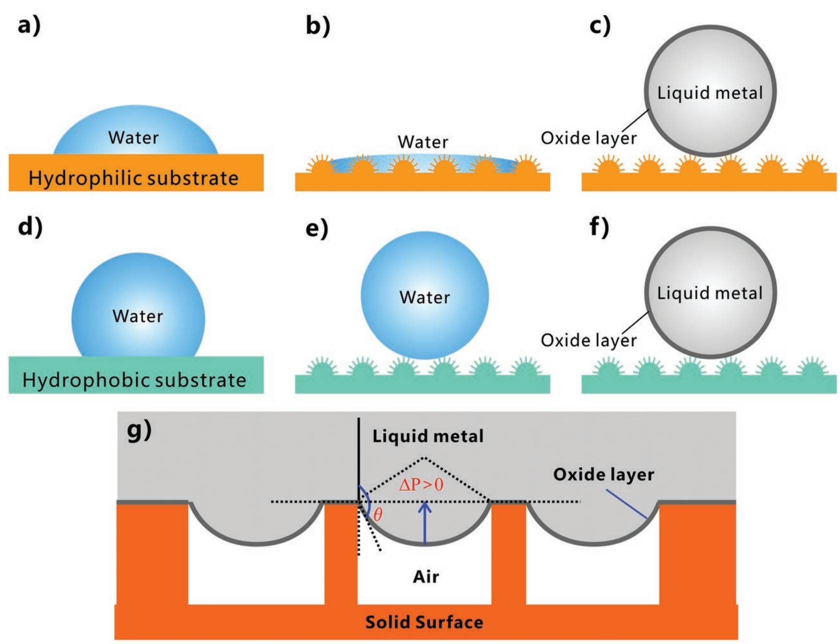

Figure 4. Wetting model of a water droplet or a LM droplet on different hydrophilic/hydrophobic substrates. a,d) Water droplet on the flat substrates. b,e) Water droplet on the fsL-induced rough surfaces. c,f) LM droplet on the fsL-structured rough surfaces. Substrate in a–c) represents hydrophilic materials such as Si while substrate in d–f) represents hydrophobic materials such as PDMS. g) LM on the substrate with uniform circular deep holes.

LM and solid, controlling the shape of LM, designing LM pattern. For example, when a liquid robot made up of LM walks or even jumps on a supermetalphobic surface, the robot does not worry about that its feet stick on the ground, unable to move, as well as continuous volume loss caused by the adhesion-induced residues on every footprint (**Figure 5**a,b). Since the flat surface has high adhesion to LM while supermetalphobic microstructure has strong LM repellence, LM can be easily printed on the high adhesive area of a patterned surface that is composed of both untreated flat domain and supermetalphobic domain (Figure 5c). LM has the features of high conductivity, great flexibility, and strong ductility, so the obtained LM pattern can act as a soft circuit in flexible electronics (Figure 5d).

FsL pulses have the characteristics of extremely short pulse width and ultrahigh peak intensity, which allow fsL processing to become an important tool in advanced nano/microfabrication nowadays.[30–33] Importantly, fsL can process almost all of the known materials, thereby micro/nanoscale surface structure can be created on any substrates by direct fsL processing.[59–66] In the process of treating a solid surface by fsL pulses, nonlinear absorption results in the occurrence of multiphoton/avalanche ionization.[67–70] Part energy of fsL pulses is absorbed by electrons and finally transferred into the material. Usually, plasma with extremely high pressure and high temperature generates at the ablation spot. As the plasma expands and bursts out, the ionized surface materials are removed away. The ablation-induced material removal causes a permanent damage of substrate surface, leading to rough surface microstructure. The primal microstructure is further roughed by the re-solidification of the fallen ejected molten particles. Every material can be ablated by fsL and its surface can be easily roughed. Therefore, supermetalphobicity is potentially obtained on the surfaces of various materials after fsL processing.

In conclusion, the influence of the surface chemistry and microstructure on achieving supermetalphobicity was revealed. FsL processing was utilized to prepare micro/nanoscale structures on Si and PDMS surfaces. The structured Si surface shows superhydrophilicity but superhydrophobicity after fluoroalkylsilane modification, while the structured PDMS exhibits superhydrophobicity but superhydrophilicity after oxygen plasma treatment. Interestingly, it is found that both the superhydrophobic and superhydrophilic Si/PDMS surfaces have excellent LM repellence. A LM droplet on the superhydrophilic/superhydrophobic Si surface has a MCA of 163.0 ± 3.0°/160.0 ± 2.0° and a MSA of 5.7 ± 0.7°/4.0 ± 1.0°. On the superhydrophobic/superhydrophilic PDMS surface, the LM droplet has a MCA of 158.3 ± 4.3°/161.7 ± 1.7° and a MSA of 4.0 ± 1.0°/3.3 ± 0.7°. The results indicate that both the superhydrophilic and the superhydrophobic Si/PDMS surfaces have similar supermetalphobicity; that is, the supermetalphobicity does not depend on the superhydrophobicity or superhydrophilicity for a solid substrate. Different from water wettability, the liquid/solid (LM/substrate) contact is replaced by a solid/solid (oxide layer/substrate) contact for a LM droplet on a textured solid surface. The experimental comparison and contact model analysis reveal that surface microstructure actually plays a crucial role in endowing a surface with supermetalphobicity rather than surface chemistry. We believe that the established principle for endowing any materials with remarkable repellence to LMs has important significance, which will accelerate the application progress of LM materials in flexible circuits and liquid robots.

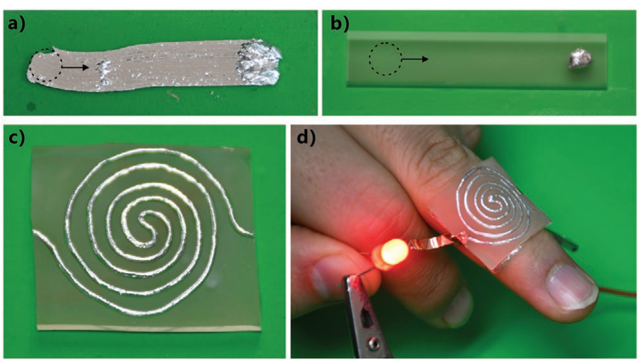

Figure 5. Potential applications of the fsL-induced supermetalphobic microstructure. LM robot walking (from left to right) on a) the untreated PDMS surface and b) the supermetalphobic PDMS surface. The black dotted circle shows the starting position. Footprint was clearly marked on the untreated PDMS surface, while there was no footprint left on the supermetalphobic PDMS surface. c) LM pattern printed on the surface composed of both untreated flat domain and supermetalphobic domain. d) Application of the LM pattern as a flexible circuit.

Experimental Section

Materials: The used Si substrate is single crystal p-type (100). The PDMS sheet was obtained through mixing the prepolymer and curing agent (DC-184) at the volume ratio of 10:1. Then, the liquid mixture was cured at 80 °C for 2 h. The typical EgaIn (70% Ga & 30% In) (Shuochen Metal Co., Ltd., China) droplet was adopted in the experiment as the LM. Liquid EGaIn has the melting point of ≈15.5 °C, surface tension of $\approx 624 \times 10^{-3}$ N m^{-1}, viscosity of $\approx 1.99 \times 10^{-3}$ Pa·s, conductivity of $\approx 3.40 \times 10^{6}$ S m^{-1}, thermal conductivity of ≈26.6 W m^{-1} K^{-1}, and density of 6.28 g cm^{-3}.[71]

Femtosecond Laser Treatment: FsL was applied to generate microstructure on the sample surfaces. The sample was previously fixed on a moveable platform. Then, the fsL beam (with the pulse width of 50 fs, center wavelength of 800 nm, and repetition frequency of 1 KHz) was focused on the sample surface via an objective lens and ablated the sample under the line-by-line (serial) scanning manner. The Si surface and PDMS surface was ablated by fsL (with a constant power of 20 mW) at the scanning speed of 2 and 4 mm s^{-1} and the scanning space of 2 and 4 µm, respectively. The laser fluence for ablating Si and PDMS is 1.79 and 3.18 J cm^{-1}. Finally, the samples were ultrasonically cleaned with alcohol and deionized water.

Surface Chemical Modification: To switch the SFE of Si substrate from high to low, the Si sample was soaked in a 0.5% fluoroalkylsilane solution (1*H*,1*H*,2*H*,2*H*-heptadecafluorodecyltrimethoxysilane) in ethanol for 12 h. As the fluoroalkylsilane monolayer was successfully grafted onto the Si surface, the wettability of Si surface switched from hydrophilicity to hydrophobicity. By contrast, the PDMS was treated by oxygen plasma at the power of 50 W for 30 s to activate its surface. As a result, the SFE of the PDMS surface was switched from low to high, enabling its wettability to switch from hydrophobicity to hydrophilicity.

Walk of Liquid Robot: A big LM droplet mixed with iron powers was adopted as a liquid "robot," whose movement could be controlled by a magnet. The liquid robot was driven by the magnetic field to move from one side of the sample surfaces to another.

Preparation of the LM-Based Flexible Circuit: The PDMS surface was selectively ablated by fsL, enabling that the surface was composed of both the untreated flat domain and the structured domain. A pattern of untreated area, surround by rough microstructure, was obtained, whose shape could be designed during selective fsL processing. As the flat surface had high adhesion to LM while microstructure had strong LM repellence, LM could be printed on the patterned area, resulting in a LM pattern. Such LM pattern can act as a flexible circuit.

Characterization: The morphology of the fsL-ablated sample surfaces was obtained by a SEM (FlexSEM-1000). The wettabilities (i.e., contact angle and sliding angle) of water and LM droplets on the sample surfaces were measured by a contact-angle meter (JC2000D). The adhesive force between solid substrates and LM droplet was the critical force that allowed the LM droplet to detach from the substrates, which was investigated through a high-sensitivity microelectromechanical balance system (Data-Physics DCAT 11).[72–74] A LM droplet (about 10 µL) was suspended on a metal ring and the sample was placed on the balance platform. The sample was slowly moved upward until it touched the LM droplet. Then, the sample was moved down. The balance force gradually increased, and reached a maximum before the droplet detached from the sample. The peak data recorded in the force–distance curve was taken as the maximum adhesive force.

Acknowledgements

This work was supported by the National Key Research and Development Program of China under the Grant no. 2017YFB1104700, the National Science Foundation of China under the Grant nos. 61805192, 61875158, U1630111, and 61435005, and the Fundamental Research Funds for the Central Universities.

Conflict of Interest

The authors declare no conflict of interest.

Author Contributions

J.Y. designed the experiments and wrote the manuscript. C.Z. characterized the wettability to liquid metal droplet. X.B. characterized the wettability to water droplet. F.C. directed and supervised the research. Other authors contributed toward significant discussions and revised the paper.

Keywords

eutectic gallium–indium, femtosecond laser processing, liquid–metal repellence, superhydrophobicity, supermetalphobicity

Received: November 15, 2019
Revised: January 3, 2020
Published online: February 5, 2020

[1] L. Sheng, Z. He, Y. Yao, J. Liu, *Small* **2015**, *11*, 5253.
[2] J. Zhang, Y. Yao, L. Sheng, J. Liu, *Adv. Mater.* **2015**, *27*, 2648.
[3] J. Wang, G. Cai, S. Li, D. Gao, J. Xiong, P. S. Lee, *Adv. Mater.* **2018**, *30*, 1706157.
[4] M. G. Mohammed, R. Kramer, *Adv. Mater.* **2017**, *29*, 1604965.
[5] B. J. Carey, J. Z. Ou, R. M. Clark, K. J. Berean, A. Zavabeti, A. S. Chesman, S. P. Russo, D. W. Lau, Z. Q. Xu, Q. Bao, O. Kevehei, B. C. Gibson, M. D. Dickey, R. B. Kaner, T. Daeneke, K. Kalantar-Zadeh, *Nat. Commun.* **2017**, *8*, 14482.
[6] M. D. Dickey, *Adv. Mater.* **2017**, *29*, 1606425.
[7] Y.-H. Wu, S.-T. Xing, R.-M. Zheng, S.-Q. Liu, Z.-F. Deng, H.-Z. Liu, P.-P. Wang, L. Liu, *J. Mater. Chem. C* **2018**, *6*, 6755.
[8] T. Lu, L. Finkenauer, J. Wissman, C. Majidi, *Adv. Funct. Mater.* **2014**, *24*, 3351.
[9] A. Hirsch, L. Dejace, H. O. Michaud, S. P. Lacour, *Acc. Chem. Res.* **2019**, *52*, 534.
[10] T. Daeneke, K. Khoshmanesh, N. Mahmood, I. A. de Castro, D. Esrafilzadeh, S. Barrow, M. Dickey, *Chem. Soc. Rev.* **2018**, *47*, 4073.
[11] N. Kazem, T. Hellebrekers, C. Majidi, *Adv. Mater.* **2017**, *29*, 1605985.
[12] D. Kim, P. Thissen, G. Viner, D. W. Lee, W. Choi, Y. J. Chabal, J. B. Lee, *ACS Appl. Mater. Interfaces* **2013**, *5*, 179.
[13] K. Doudrick, S. Liu, E. M. Mutunga, K. L. Klein, V. Damle, K. K. Varanasi, K. Rykaczewski, *Langmuir* **2014**, *30*, 6867.
[14] D. Kim, Y. Lee, D.-W. Lee, W. Choi, K. Yoo, J.-B. Lee, *Sens. Actuators, B* **2015**, *207*, 199.
[15] N. Ilyas, A. Cook, C. E. Tabor, *Adv. Mater. Interfaces* **2017**, *4*, 1700141.
[16] I. D. Joshipura, H. R. Ayers, G. A. Castillo, C. Ladd, C. E. Tabor, J. J. Adams, M. D. Dickey, *ACS Appl. Mater. Interfaces* **2018**, *10*, 44686.
[17] S. S. Kadlaskar, J. H. Yoo, Abhijeet, J. B. Lee, W. Choi, *J. Colloid Interface Sci.* **2017**, *492*, 33.
[18] Y. Jiang, S. Su, H. Peng, H. S. Kwok, X. Zhou, S. Chen, *J. Mater. Chem. C* **2017**, *5*, 12378.
[19] R. K. Kramer, J. W. Boley, H. A. Stone, J. C. Weaver, R. J. Wood, *Langmuir* **2014**, *30*, 533.
[20] L. Feng, S. Li, Y. Li, H. Li, L. Zhang, J. Zhai, Y. Song, B. Liu, L. Jiang, D. Zhu, *Adv. Mater.* **2002**, *14*, 1857.
[21] V. Zorba, E. Stratakis, M. Barberoglou, E. Spanakis, P. Tzanetakis, S. H. Anastasiadis, C. Fostas, *Adv. Mater.* **2008**, *20*, 4049.
[22] J. Yong, F. Chen, Y. Fang, J. Huo, Q. Yang, J. Zhang, H. Bian, X. Hou, *ACS Appl. Mater. Interfaces* **2017**, *9*, 39863.
[23] J.-N. Wang, Y.-L. Zhang, Y. Liu, W. Zheng, L. P. Lee, H.-B. Sun, *Nanoscale* **2015**, *7*, 7101.
[24] J. Yong, F. Chen, Q. Yang, J. Huo, X Hou, *Chem. Soc. Rev.* **2017**, *46*, 4168.
[25] Y. Tian, B. Su, L. Jiang, *Adv. Mater.* **2014**, *26*, 6872.
[26] L. Wen, Y. Tian, L. Jiang, *Angew. Chem., Int. Ed.* **2015**, *54*, 3387.
[27] M. Liu, S. Wang, L. Jiang, *Nat. Rev. Mater.* **2017**, *2*, 17036.
[28] B. Su, Y. Tian, L. Jiang, *J. Am. Chem. Soc.* **2016**, *138*, 1727.
[29] X. Hao, P. Sun, S. Xiao, Y. Yang, L. Li, *Appl. Surf. Sci.* **2020**, *151*, 144288.
[30] T. C. Chong, M. H. Hong, L. P. Shi, *Laser Photonics Rev.* **2010**, *4*, 123.
[31] K. Sugioka, Y. Cheng, *Appl. Phys. Rev.* **2014**, *1*, 041303.
[32] K. Sugioka, Y. Cheng, *Light: Sci. Appl.* **2014**, *3*, e149.
[33] A. Y. Vorobyev, C. Guo, *Laser Photonics Rev.* **2013**, *7*, 385.
[34] J. Yong, F. Chen, Q. Yang, X. Hou, *Soft Mater* **2015**, *11*, 8897.
[35] J. Yong, F. Chen, Q. Yang, Z. Jiang, X. Hou, *Adv. Mater. Interfaces* **2018**, *5*, 1701370.
[36] J. Yong, Q. Yang, C. Guo, F. Chen, X. Hou, *RSC Adv.* **2019**, *9*, 12470.
[37] D. Zhang, F. Chen, Q. Yang, J. Yong, H. Bian, Y. Ou, J. Si, X. Meng, X. Hou, *ACS Appl. Mater. Interfaces* **2012**, *4*, 4905.
[38] F. Chen, D. Zhang, Q. Yang, X. Wang, B. Dai, X. Li, X. Hao, Y. Ding, J. Si, X. Hou, *Langmuir* **2011**, *27*, 359.
[39] J. Yong, F. Chen, Q. Yang, D. Zhang, U. Farooq, G. Du, X. Hou, *J. Mater. Chem. A* **2014**, *2*, 8790.
[40] J. Yong, Q. Yang, F. Chen, H. Bian, G. Du, U. Farooq, X. Hou, *Adv. Mater. Interfaces* **2015**, *2*, 1400388.
[41] J. Yong, Q. Yang, F. Chen, D. Zhang, H. Bian, Y. Ou, J. Si, G. Du, X. Hou, *Appl. Phys. A* **2013**, *111*, 243.
[42] J. Yong, F. Chen, Q. Yang, D. Zhang, H. Bian, G. Du, J. Si, X. Meng, X. Hou, *Langmuir* **2013**, *29*, 3274.

[43] J. Yong, F. Chen, Q. Yang, D. Zhang, G. Du, J. Si, F. Yun, X. Hou, *J. Phys. Chem. C* **2013**, *117*, 24907.
[44] J. Yong, Q. Yang, F. Chen, D. Zhang, U. Farooq, G. Du, X. Hou, *J. Mater. Chem. A* **2014**, *2*, 5499.
[45] J. Yong, F. Chen, J. Huo, Y. Fang, Q. Yang, J. Zhang, X. Hou, *Nanoscale* **2018**, *10*, 3688.
[46] J. Yong, Q. Yang, F. Chen, D. Zhang, G. Du, H. Bian, J. Si, F. Yun, X. Hou, *Appl. Surf. Sci.* **2014**, *288*, 579.
[47] D. Wu, S. Wu, Q.-D. Chen, S. Zhao, H. Zhang, J. Jiao, J. A. Piersol, J.-N. Wang, H.-B. Sun, L. Jiang, *Lab Chip* **2011**, *11*, 3873.
[48] Y. Cai, L. Lin, Z. Xue, M. Liu, S. Wang, L. Jiang, *Adv. Funct. Mater.* **2014**, *24*, 809.
[49] M. Morra, E. Occhiello, R. Marola, F. Garbassi, P. Humphrey, D. Johnson, *J. Colloid Interface Sci.* **1990**, *137*, 11.
[50] H. Hillborg, J. F. Ankner, U. W. Gedde, G. D. Smith, H. K. Yasuda, K. Wikström, *Polymer* **2000**, *41*, 6851.
[51] J. Yong, F. Chen, M. Li, Q. Yang, Y. Fang, J. Huo, X. Hou, *J. Mater. Chem. A* **2017**, *5*, 25249.
[52] J. Yong, S. C. Singh, Z. Zhan, F. Chen, C. Guo, *Langmuir* **2019**, *35*, 921.
[53] J. Genzer, K. Efimenko, *Biofouling* **2006**, *22*, 339.
[54] R. N. Wenzel, *Ind. Eng. Chem.* **1936**, *28*, 988.
[55] A. B. D. Cassie, S. Baxter, *Trans. Faraday Soc.* **1994**, *40*, 546.
[56] J. P. Youngblood, T. J. McCarthy, *Macromolecules* **1999**, *32*, 6800.
[57] Z. Chen, J. Wang, H. Lai, Y. Du, R. Hou, C. Li, N. Zhang, K. Sun, *Langmuir* **2015**, *31*, 1393.
[58] E. Zhang, Z. Cheng, T. Lv, Y. Qian, Y. Liu, *J. Mater. Chem. A* **2015**, *3*, 13411.
[59] Y. Zhang, Y. Li, Y. Hu, X. Zhu, Y. Huang, Z. Zhang, S. Rao, Z. Hu, W. Qiu, Y. Wang, G. Li, L. Yang, J. Li, D. Wu, W. Huang, C. Qiu, J. Chu, *Adv. Mater.* **2018**, *30*, 1803072.
[60] Y. Jiao, C. Li, X. Lv, Y. Zhang, S. Wu, C. Chen, Y. Hu, J. Li, D. Wu, J. Chu, *J. Mater. Chem. A* **2018**, *6*, 20878.
[61] J. Yong, S. C. Singh, Z. Zhan, F. Chen, C. Guo, *ACS Appl. Mater. Interfaces* **2019**, *11*, 8667.
[62] G. Li, H. Fan, F. Ren, C. Zhou, Z. Zhang, B. Xu, S. Wu, Y. Hu, W. Zhu, Y. Zeng, X. Li, J. Chu, D. Wu, *J. Mater. Chem. A* **2016**, *4*, 18832.
[63] X. Bai, Q. Yang, Y. Fang, J. Zhang, J. Yong, X. Hou, F. Chen, *Chem. Eng. J.* **2020**, *383*, 123143.
[64] Q. Li, Q. Wu, Y. Li, C. Zhang, Z. Jia, J. Yao, J. Sun, J. Xu, *Photonics Res.* **2018**, *6*, 789.
[65] K. Xu, C. Zhang, R. Zhou, R. Ji, M. Hong, *Opt. Express* **2016**, *24*, 10352.
[66] J. Yong, S. C. Singh, Z. Zhan, M. EIKabbash, F. Chen, C. Guo, *ACS Appl. Nano Mater.* **2019**, *2*, 7362.
[67] D. B. Wolfe, J. B. Ashcom, J. C. Hwang, C. B. Schaffer, E. Mazur, G. M. Whitesides, *Adv. Mater.* **2003**, *15*, 62.
[68] J. Bonse, S. Baudach, J. Krüger, W. Kautek, M. Lenzner, *Appl. Phys. A* **2002**, *74*, 19.
[69] M. Zhou, H. F. Yang, B. J. Li, J. Dai, J. K. Di, E. L. Zhao, L. Cai, *Appl. Phys. A* **2009**, *94*, 571.
[70] J. Yong, J. Huo, Q. Yang, F. Chen, Y. Fang, X. Wu, L. Liu, J. Zhang, X. Hou, *Adv. Mater. Interfaces* **2018**, *5*, 1701479.
[71] L. Zhu, B. Wang, S. H. Wang, X. Zhou, *Small* **2020**, https://doi.org/10.1002/smll.201903841.
[72] M. Liu, S. Wang, Z. Wei, Y. Song, L. Jiang, *Adv. Mater.* **2009**, *21*, 665.
[73] D. Wu, S.-Z. Wu, Q.-D. Chen, Y.-L. Zhang, J. Yao, X. Yao, L. G. Niu, L. Jiang, H.-B. Sun, *Adv. Mater.* **2011**, *23*, 545.
[74] Y. Lai, X. Gao, H. Zhuang, J. Huang, C. Lin, L. Jiang, *Adv. Mater.* **2009**, *21*, 3799.